DOI 10.1016/j.molcatb.2017.01.009

The immobilisation of proteases produced by SSF onto functionalized magnetic nanoparticles: Application in the hydrolysis of different protein sources

Noraziah Abu Yazid, Raquel Barrena, and Antoni Sánchez*

Composting Research Group

Department of Chemical, Biological and Environmental Engineering

Escola d'Enginyeria

Universitat Autònoma de Barcelona

08193-Bellaterra (Barcelona, Spain)

*Corresponding author:

Tel.: +34 935811019

Fax: +34 935812013

Email address: antoni.sanchez@uab.cat

ABSTRACT

Alkaline proteases produced from protein-rich waste (hair waste and soya residues) by solid state fermentation (SSF) were immobilised onto functionalized magnetic iron oxide nanoparticles (MNPs) using glutaraldehyde as a crosslinking agent. The covalent binding method had a better immobilisation yield compared to simple adsorption, retaining 93%-96% (459±106 U/mg nanoparticles, 319±34 U/mg nanoparticles) of hair waste and soya residues proteases, respectively after crosslinking with 5% glutaraldehyde for 6 h. However, the adsorption immobilisation yield was 47%-54% after 8 h for both proteases. MNPs and immobilised proteases were characterized using transmission electron microscopy (TEM), scanning electron microscopy (SEM), Fourier transform infrared spectroscopy (FT-IR) and electron diffraction. Our results indicated successful crosslinking between the proteases and amino-functionalized MNPs. The operational stability (pH and temperature) and storage stability of free and immobilised enzyme were also analysed. Despite the fact that the optimum pH of free and immobilised proteases was identical in the alkaline region, the immobilised proteases reached their optimum condition at higher temperatures (~~40ºC – 60ºC~~ 40 ºC – 60 ºC). After 2 months of storage at ~~4ºC~~ 4 ºC, the immobilised proteases showed good stability, retaining more than 85% of their initial activity. The high magnetic response of MNPs render an ease of separation and reusability, which contributes to the residual activity of both immobilised proteases on MNPs ~~remained~~ retaining more than 60% of their initial values after seven hydrolytic cycles. These results ~~resulted~~ showed the enhancement of the stability of the crosslinking interactions between the proteases and nanoparticles. The immobilised proteases were capable of hydrolysing ~~select~~ selected proteins (casein, oat bran protein isolate, and egg white albumin). However, differences in the degree of hydrolysis were observed, depending on the combination of the protease and type of substrate used.

Keywords: protease; protein-rich waste; solid state fermentation; hydrolysis; immobilisation

1. Introduction

Because of the proteolytic nature of alkaline proteases, they have been commercially utilised for industrial applications, explicitly in the food, pharmaceutical, textile, detergent, and leather industries [1,2]. Their specific role in protein hydrolysis has drawn worldwide attention regarding the versatility of these enzymes for biotechnological applications. Currently, the general cost of protease production is very high, considering the cost of substrates, commercial media and maintenance of cultures used for inoculation. For this reason, the need to develop novel processes with higher yields is highly recommended from a commercial point of view [3].

Different options have been considered to reduce the cost and increase the utilization of proteases. One of the most promising alternatives is solid state fermentation (SSF), which allows the procurement of value-added products using inexpensive waste as a solid substrate. SSF has been successfully applied in the production of proteases using protein-rich waste without the need to inoculate a specific microorganism [4,5]. In addition to recycling the abundant solid waste produced by industries as cheap substrates, SSF avoids the hassle of maintaining cultures since microorganism can develop mutations over time [6]. Economically, no additional cost is required, as there is no restricted sterilized environment required to produce proteases through SSF since a specific microorganism for inoculation is not involved.

Apart from that, soluble proteases are susceptible to autolysis, which leads to their rapid inactivation. The instability and lack of flexibility, reusability and recovery make their use a challenge for commercialization. Therefore, the use of immobilisation enzymes offers an attractive method in which immobilised enzymes have enhanced stability that allows for their recyclability and simple recovery without contamination of the final product [7]. There are

five basic enzyme immobilisation methods, including simple adsorption, covalent binding, encapsulation, crosslinking, and entrapment [8].

~~Of all the methods, covalent binding provides firm binding between the enzyme and carrier and avoids enzyme, as it can be regulated by using specific functional groups (NH_2, -SH) to bind with the proteins.~~ Of all the methods, covalent binding provides firm binding between the enzyme and carrier, thus avoiding enzyme leakage as it can be regulated by using specific functional groups (-NH_2, -SH) [9]. This method of immobilisation provides an efficient way to increase the stability and flexibility of enzyme reusability and recovery [10]. Coupling agents, such as glutaraldehyde, maleic anhydride and genipin, have been widely used as their functional groups can interact with the functional groups of modified carriers and proteins [10,11]. Glutaraldehyde can be used either to alter enzymes after immobilisation or to activate the support for enzyme immobilisation. In addition, the use of glutaraldehyde can increase protein stability, thus avoiding protease autolysis [2,12].

In recent years, the immobilisation of enzymes onto nanomaterials, particularly iron oxide magnetic nanoparticles (MNPs), to form nanobiocatalysts has attracted much attention in some fields of research, including biolabeling, bioseparation, biosensors, biofuel cells, and environmental analysis [9,13]. The use of MNPs has been particularly attractive for immobilisation because of their special characteristics, such as their high surface area, simple manipulation and separation by the application of an external magnetic field, biocompatibility, biodegradability, and low toxicity [10,14]. There are several studies reporting the application of purified protease immobilised on magnetic supports [15–18]; however there are only a few studies that have exploited MNPs for crude protease immobilisation and further use in protein hydrolysis and synthesis [19].

In this work, the use of relatively inexpensive enzyme preparative for immobilisation onto functionalized MNPs and crosslinking with glutaraldehyde was assessed. The goal was

to test the viability of using low-cost proteases derived from animal (hair waste) and vegetable (soy fibre residues) protein-rich waste that were produced by SSF after being immobilised onto functionalized MNPs in the hydrolysis of different type of proteins. The relative differences in terms of stability and reusability between the free and immobilised enzymes were significant, exhibiting the feasibility of the immobilised enzymes produced in this work. Also, the magnetic properties of the support render a convenient separation between the substrate and the enzymes within the catalytic system.

2. Materials and Methods

2.1 Material and reagents

Ferric chloride ($FeCl_3 \cdot 6H_2O$), ferrous sulphate ($FeSO_4 \cdot 7H_2O$), (3-aminopropyl)-triethoxysilane (3-APTES, 97%), glutaraldehyde solution (50%), cetyl-trimethyl-ammonium bromide (CTAB), trichloroacetic acid (TCA), Folin-Ciocalteu reagent, casein from bovine milk, and egg white albumin were obtained from Sigma-Aldrich (Spain). Oat bran containing 17.6% protein was purchased from a supermarket (Mercadona, Spain). Hair waste with a protein content of 75.6% was obtained from the local tanning industry located in Igualada, Barcelona, and soya fibre residues with a protein content of 25.1% were received from Natursoy, Spain. β-mercaptoethanol, tricine sample buffer, 10%-20% Mini-PROTEAN gels, and Coomassie 250 stain were purchased from Bio-Rad (Spain). All other chemicals were from commercial sources and were of analytical grade.

2.2 Preparation of the protease enzyme concentrates from protein-rich waste using SSF

Two different sources of alkaline proteases were produced from protein-rich waste, hair waste and soya fibre residues using solid state fermentation (SSF) as described elsewhere [4,5]. Briefly, hair waste and soya fibre residues were individually mixed with anaerobically

digested sludge at a weight ratio of 1:2, and then, the mixtures were added to a bulking agent (wood chips) at a volumetric ratio of 1:1. SSF was undertaken in triplicate using 10 L air-tight reactors for approximately 1 to 3 weeks. Later, the proteases, Phw from hair waste and Psr from soya fibre residues, were extracted from the reactors using Tris-HCl buffer (50 mM, pH 8.1). The times for extracting proteases for different substrates were specified for each case based on the maximum activity of the protease produced during SSF. Phw at day 14th yielded 787±124 U/g DW, and Psr at day 4th yielded 634±24 U/g DW. The extracts were ultrafiltrated through Amicon Ultra-15 centrifugal filter devices (Millipore, Ireland) with a 10kDa molecular weight cut-off (MWCO) prior to lyophilisation. The initial activities after lyophilisation for Phw and Psr were 466 U/ml and 330 U/ml, respectively.

2.3 Preparation of oat bran protein isolate (OBPI)

The preparation of oat bran protein isolate (OBPI) was performed as described elsewhere [20] with slight modifications. Briefly, oat bran was added to 1.0 M NaCl at a ratio of 1:8 (w/v), and the pH was adjusted to 9.5 using 1.0 M NaOH. The mixture was agitated for 30 min at room temperature. Then, the supernatant was collected after centrifuged at 5,000 x g for 25 min at ~~4ºC~~ 4 ºC. The pH was adjusted to 4 with 1.0 M HCl prior to centrifugation at 5,000 x g for 40 min at ~~4ºC~~ 4 ºC. The supernatant was then discarded, and the protein isolate was dissolved in Milli-Q water and adjusted to pH 7 with 0.1 M NaOH. The protein isolate was lyophilised and stored at ~~-20ºC~~ -20 ºC for future use.

2.4 Synthesis of amino-functionalized Fe_3O_4 magnetic nanoparticles (MNPs)

Magnetic nanoparticles (MNPs) were synthesised by co-precipitation in water phase [21,22] with slight modifications. A mixture of 25 mM ferrous sulphate and 50 mM of ferric chloride were dissolved in 100 ml of Milli-Q water with the addition of 0.1% of CTAB as a stabiliser. The mixture was stirred at ~~40ºC~~ 40 ºC for 1 hour under ~~a~~ the nitrogen atmosphere.

Then, 125 ml of deoxygenated NaOH (0.5 M) was added dropwise to the mixture, and the mixture was left for 1 hour at ~~40ºC~~ 40 ºC to let the solution chemically precipitate. The resultant MNPs were separated magnetically and washed five times with Milli-Q water. The recovered MNPs were dried overnight at ~~60ºC~~ 60 ºC.

The surface of the MNPs was modified using a silanization reaction. Approximately 0.61 g of MNPs was dispersed in a solution containing 3.05 ml of APTES, 0.763 ml of Milli-Q water, and 45.75 ml of methanol. The mixture was ultrasonically agitated for 30 min. Then, 10 ml of glycerol was added and heated at ~~90ºC~~ 90 ºC for 6 h, and the mixture was stirred until separation. The surface-modified MNPs were recovered by applying a magnet, and they were washed three times with Milli-Q water.

2.5 Immobilisation of alkaline proteases (Phw, Psr)

~~For immobilisation of surface modified MNPs, 1 ml of alkaline protease from hair waste (Phw) with an initial activity 466 U/ml or alkaline protease from soya residue (Psr) with an initial activity 330 U/ml was dispersed in 9 ml of Tris HCl buffer (pH 8.1) and mixed with 100 mg of amino functionalized MNPs. The activation of the NH_2 groups in the nanoparticles was carried out by adding glutaraldehyde as a crosslinking agent at various concentrations (1%, 2.5%, and 5% (v/v)). The mixture was gently agitated at 4ºC 4 ºC for 8 h. Subsequently, the immobilised proteases were separated by a magnetic field, washed five times with Tris buffer (50 mM, pH 8.1) to remove any unbound glutaraldehyde and finally resuspended in 1 ml of Tris buffer (50 mM, pH 8.1). The immobilised proteases were stored at 4ºC 4 ºC for future use.~~

To begin with immobilisation of protease onto surface-modified MNPs, 1 ml of alkaline protease from hair waste (Phw) with an initial activity 466 U/ml and alkaline protease from soya residue (Psr) with an initial activity 330 U/ml, respectively, was dissolved in 9 ml of Tris-HCl buffer (pH 8.1). Then, 100 mg of amino-functionalized MNPs was dispersed into

the mixture. Afterwards, the activation of the NH_2 groups in the nanoparticles was carried out by adding glutaraldehyde as a crosslinking agent at various concentrations (1%, 2.5%, and 5% (v/v)) in the mixtures, followed by gentle agitation at 4 ℃ for 8 h. Subsequently, the MNPs with the immobilised proteases (MNPs-protease) were separated by a magnetic field and washed five times with Tris buffer (50 mM, pH 8.1) to remove any unbound glutaraldehyde and enzyme. Finally, the MNPs-protease were resuspended in 1 ml of Tris buffer (50 mM, pH 8.1) and stored at 4 ℃ for further application.

For immobilisation via adsorption, approximately 100 mg of naked MNPs were dispersed in 9 ml of the Tris buffer solution (50 mM, pH 8.1). Then, 1 ml of free alkaline protease from hair waste (466 U/ml) or soya residue (330 U/ml) was added. The mixture was gently agitated at ~~4℃~~ 4 ℃ for 8 h. Later, the immobilised proteases were magnetically separated and treated as previously described.

The immobilisation yield (%) and the amount of immobilised protease (Phw_im, Psr_im) loading on MNPs (U/mg) were calculated using following equations (Eqs. 1, 2) [15,23]:

$$Enzyme\ loading\ (U/mg) = (U_i - U_{sp})/W \quad (1)$$

$$Immobilisation\ yield\ (\%) = \left(U_i - U_{sp}\right)/U_i \times 100 \quad (2)$$

Where U_i is the initial enzyme activity (U), U_f is the enzyme activity in the supernatant after immobilisation (U), and W is the weight of MNPs used for immobilisation (mg). Furthermore, the immobilisation efficiency (%) and activity recovery (%) were calculated as follows (Eqs. 3, 4) [23]:

$$Efficiency\ (\%) = (U_e/U_{imm}) \times 100 \quad (3)$$

$$Activity\ recovery\ (\%) = (U_e/U_i) \times 100 \quad (4)$$

Where U_e is the activity of bound enzyme that is measured in the immobilisate (U), U_{imm} is the immobilised enzyme activity determined from subtracting the remaining enzyme activity in the supernatant from the initial activity (U).

2.6 Characterization of the immobilised enzymes

Functionalized MNPs before and after immobilisation were characterized using high resolution transmission electron microscopy (HRTEM, JEM-2011/JEOL) and scanning electron microscopy (SEM, Zeiss Merlin). The samples were prepared by placing a drop of the sonicated solutions on a copper grid, and then, the samples were allowed to dry. Samples with the immobilised enzyme were stained with uranyl acetate (2%) prior to analysis. Functionalized nanoparticle immobilisation was then confirmed using Fourier Transform Infrared spectroscopy (FT-IR, Bruker Tenser 27) within a range of 500-4,000 cm^{-1}.

2.7 Stability of immobilised protease

The storage stability was determined by maintaining the immobilised enzymes via crosslinking and simple adsorption at ~~4ºC~~ 4 ºC for 60 days. The activity of the enzymes was measured at day 0^{th} as the initial activity, while the activity for the 60^{th} and 7^{th} days were used as the final activity of the immobilised enzymes and free enzymes, respectively.

To study the operational stability, both immobilised and free enzymes were incubated for 1 h at various pH and temperature values according to the response surface of the central composite design (CCD) performed using the Design-Expert software (version 6.0.6). The CCD consisted of 13 experimental points, including five replications at the central point and four star points ($\alpha = 1$). The pH was adjusted using the following buffers: acetic acid-sodium acetate 1 M (pH 5), Tris-HCl 1 M (pH 8), and Na_2HPO_4-NaOH 0.05 M (pH 11). Analysis of variance (ANOVA) was conducted to determine the significance of the main effects.

~~The residual activity of each factor tested was calculated by that assuming the initial activity of the immobilised or free enzyme was 100%.~~ The residual activity of each factor was calculated by assuming that the initial activity of the immobilised or free enzyme is 100%.

2.8 Reusability of immobilised protease

The reusability of immobilised proteases from hair waste (Phw) and soya fibre residue (Psr) was tested on casein as a model protein. The initial activities of the immobilised enzymes were measured and compared with seven consecutive repeated uses of immobilised enzymes under the assay conditions. After each cycle, immobilised enzymes were magnetically separated and washed with Tris-HCl buffer (50 mM, pH 8.1). Then, they were resuspended in fresh medium and incubated at ~~50ºC~~ 50 ºC for 120 min. The activity of immobilised enzymes from the first batch was considered to be 100%.

2.9 Application of immobilised proteases in protein hydrolysis

Prior to hydrolysis, 4% (w/v) suspension of selected proteins (casein from bovine milk, egg white albumin, and OBPI) in Tris-HCl buffer (50 mM, pH 8.1) were incubated at ~~50ºC~~ 50 ºC for 15 min. Then, the reaction was initiated by adding 1 ml of free enzymes (330-460 U/ml) or 1 ml immobilised enzymes suspension (319-459 U/mg NP) into 9 ml of substrate. The mixture was incubated in a water bath at ~~50ºC~~ 50 ºC with mechanical agitation at 100 rpm. An aliquot of ~~six~~ 6 ml was withdrawn at 0.5, 2, 4, 6, and 24 h. The free enzyme activity was deactivated by heating the samples in boiling water for 15 min. Then, the samples were cooled by placing the samples in a cold water bath for 15 min. Afterwards, the samples were centrifuged at 5,000 x g for 15 min to separate any impurities or enzyme from the hydrolysate. The immobilised enzyme was separated from the hydrolysate by a magnetic drive. The hydrolysate was kept frozen at ~~-80ºC~~ 80 ºC prior to lyophilisation.

2.10 Analytical methods

2.10.1 Protease assay

The proteolytic activity of the free and immobilised protease was determined using casein as a substrate according to method described by Alef and Nannipieri [24] with slight modifications. Briefly, 1 ml of the enzyme extract (free enzyme) or 0.1 g of immobilised protease in 0.9 ml of Tris buffer (pH 8.1) was added to 5 ml of a 2% (w/v) casein solution and incubated at ~~50ºC~~ 50 ºC and 100 rpm for 1 hour. The reaction was terminated by adding 5 ml of 15% (w/v) TCA. The samples were centrifuged at 10,000 rpm for 10 min at ~~4ºC~~ 4 ºC. An aliquot of 0.5 ml of the supernatant was added to the alkaline reagent prior to the addition of 0.5 ml of 25% (v/v) Folin-Ciocalteu phenol reagent. The resulting solution was incubated at room temperature in the dark for 1 h. The absorbance was measured at 700 nm using a tyrosine standard. One unit of alkaline protease activity was defined as the liberation of 1 µg of tyrosine per minute under the assay conditions. All activity tests were performed in triplicate.

2.10.2 Total protein content determination

The total protein content was determined by the Lowry method [25] using bovine serum albumin (BSA) as a standard. The absorbance was analysed at 750 nm using an UV-visible spectrophotometer (Varian Cary 50).

2.10.3 Degree of hydrolysis

The degree of hydrolysis was determined by quantifying the soluble protein content after precipitation with TCA [19,26]. 1ml of protein hydrolysate was mixed with 1 ml of 10% (w/v) TCA and incubated at ~~37ºC~~ 37 ºC for 30 min to allow for precipitation. This was followed by centrifugation (10,000 x g, 10 min). Then, the soluble protein content in the

supernatant was determined by the Lowry method [25], and it was expressed in milligrams. The degree of hydrolysis (DH) was determined using the following equation (Eq.1):

$$DH(\%) = \frac{\text{soluble protein content in 10\% TCA}}{\text{total protein content}} \times 100 \quad (5)$$

2.10.4 Electrophoresis

Tricine-SDS PAGE was used to observe the pattern of smaller proteins generated after the hydrolysis reaction. Electrophoresis was performed using 10-20% Mini-PROTEAN Tris-Tricine gels under denaturing and reducing conditions. The reduction was achieved by heating the sample at ~~90ºC~~ 90 ºC for 5 min in the presence of β-mercaptoethanol (2% v/v). The gel was fixed with methanol (40% v/v) and acetic acid (10% v/v) and subsequently stained with Coomassie Brilliant Blue R-250. Then, the gel was destained with a solution containing methanol, acetic acid, and water (20: 4: 26 v/v).

3. Results and discussion

3.1 Immobilisation of Phw and Psr onto magnetic nanoparticles

The Phw and Psr enzymes from SSF were immobilised onto magnetic nanoparticles via simple adsorption and crosslinking with glutaraldehyde (GA). Both methods were carried out for 8 h with the aim of investigating the effect of time and crosslinker concentration on immobilisation (Fig. 1). The simple adsorption yielded a maximum activity recovery of 28% with an activity loading of 87±22 U/mg NP for Phw and of 33% Psr (activity loading of 70±17 U/mg NP) after 8 h of immobilisation (Fig. 1a, 1c). The immobilisation efficiency for both Phw and Psr in simple adsorption increased during 8 h with a maximum of 60-61% efficiency yield, while the maximum immobilisation yield in simple adsorption for both Phw

and Psr were 47% and 54%, respectively (Fig. 1b, 1d). The surfaces of naked MNPs likely possess high reactivity, which makes them susceptible to degradation under particular environmental conditions. This fact could involve weaker binding forces that contribute to the poor stability of the protein attachment's to the surface [9,27].

Immobilisation via the crosslinker showed good results for both enzymes studied (Phw and Psr). The immobilisation yield increased according to the increase in the GA concentration from 1%-5% up to 6 h; then, it decreased abruptly for Phw (Fig. 1b). ~~Only when 1% GA with Psr was used did the immobilisation yield continue to increase (Fig. 1b).~~ Only when using Psr with 1% GA, the immobilisation yield continues increasing (Fig. 1d). Maximum activity recovery and immobilisation yields were obtained after 6 h of crosslinking time, 90% and 96% respectively, which is (equivalent to an activity load of 459±106 U/mg NP) for Phw with 5% GA (Fig 1a, 1b). Similarly in Psr with 5% GA the maximum activity recovery and immobilisation yield were 92% and 93%, respectively (equivalent to activity loading of 319±34 U/mg NP) (Fig. 1c, 1d). In addition, the immobilisation via crosslinker was superior to simple adsorption as both of the enzymes (Phw, Psr) showed good immobilisation efficiency in the range of 45% to 98% during 6 h of immobilisation time (Fig 1b, 1d). This indicated that the crosslinking time and GA concentration play an important role during the immobilisation of enzymes in this study. As GA plays a role as a spacer arm for the carriers by providing aldehyde groups to couple to free amine groups from the enzymes, forming imines, it can also act as a denaturing agent [12]. Additionally, some studies obtained different crosslinking times (between 1 h to 4 h) and GA concentrations (from 1% to 6%), implying good biocompatibility for these specific enzymes [12,21,28,29].

3.2 Characterization of the functionalized nanoparticles used for immobilisation

Transmission electronic microscopy (TEM) images of MNPs before and after modification with APTES and after the enzymes immobilisation onto the activated surface

316 were compared (Fig. 2). The average particle size of naked MNPs slightly increased from
317 10.2 nm (Fig. 2a) to 16.1 nm (Fig. 2b) after surface modification with APTES. This effect has
318 been observed previously in other studies [30,31]. After surface modification with APTES,
319 fewer nanoparticle aggregates formed. As suggested previously [10], surface modifications of
320 magnetic nanoparticles can improve their solubility and help avoid aggregation of particles.
321 In Fig. 2c and Fig. 2d, a layer covering surface of MNPs upon immobilisation of the
322 proteases (Phw and Psr) can be seen. The thickness of this layer covering the surface of
323 MNPs was estimated to be approximately 5.1 nm for Psr and 8.4 nm for Phw, indicating an
324 increase in the size of the particles.

325 Based on electron diffraction analysis (Fig. 3) of the TEM images, the crystalline
326 structure of the particles was not affected by surface modifications. Fig. 3a shows a clear
327 loop, confirming the crystalline structure of MNPs. After surface modification by APTES or
328 CTAB as a stabilizer, the crystalline structure was not modified; however, the size of some
329 nanoparticles was enlarged, as observed in Fig. 3b and Fig. 3c. Once protease immobilisation
330 was performed, the structure of the nanoparticles became an amorphous structure, confirming
331 that the enzyme covered the surface of the nanoparticles (Fig. 3d). The surface of the naked
332 MNPs and functionalized MNPs can be observed in SEM images (Fig. 4a and Fig. 4b). The
333 small and spherical particles with well-defined edges are observed as in other studies [32]. In
334 contrast, in Fig. 4c and Fig. 4d, the edge surface of nanoparticles is smooth because they are
335 covered by the enzymes, indicating that the immobilisation of proteases onto functionalized
336 MNPs was successful.

337 The surface modification and immobilisation of proteases (Phw and Psr) onto
338 nanoparticles was confirmed by a comparison of the FT-IR spectra of naked MNPs,
339 functionalized MNPs, and Phw and Psr immobilised onto functionalized MNPs. The FT-IR
340 spectrum in Fig. 5A shows a strong absorption peak at 584 cm^{-1}, which could corresponds to

Fe-O, as indicated in other studies [33,34]. It has been suggested that this strong peak could be due to the stretching vibration mode associated with metal-oxygen absorption. In this region, the stretching vibration peaks related to metal (ferrites in particular) in the octahedral and tetrahedral sites of the oxide structure were found [31]. In Fig. 5A, the peaks at 1,662 cm^{-1} and 3,444 cm^{-1} were due to the bending and stretching vibration of -OH, respectively [35]. After grafting with APTES, the characteristic peak of the Fe-O bond shifted from 584 cm^{-1} to 638 cm^{-1} and 640 cm^{-1} because of the formation of the Fe-O-Si bond (Fig. 5B, 5C, 5D). The shifting of the absorption peaks to high wavenumbers is due to the greater electronegativity of -Si(O-) compared to H, which contributes to the bond forces for Fe-O bonds [36]. Additional strong peaks at 1,039 cm^{-1}, 1,035 cm^{-1}, and 1,034 cm^{-1} correspond to the Fe-O-Si bending vibrations, indicating that alkyl silanes are successfully attached to functionalized MNPs (Fig. 5B, 5C, 5D). Additionally, the presence of silane groups was observed at 995 cm^{-1}, 893 cm^{-1}, and 896 cm^{-1} and were from the stretching vibrations of the Si-OH and Si-O-Si groups from APTES [35,36]. Characteristic peaks of the immobilised enzymes attached via the crosslinker (Fig. 5C, 5D) were observed at 1,536 cm^{-1}, 1,544 cm^{-1} and 1,630 cm^{-1} because of the C=N and C=O absorption from the glutaraldehyde and NH_2 from the enzyme [29]. Small shifts in intensity from 2,928 cm^{-1} (Fig. 5B) to 2,991 cm^{-1} (Fig. 5C) and 2,984 cm^{-1} (Fig. 5D) correspond to the C-H stretching vibration from the methyl group [37], which illustrated the effect before and after the immobilisation of the enzymes. Additionally, in Fig. 5C and Fig. 5D, there were broad and strong peaks at 3,325 cm^{-1} and 3,344 cm^{-1}, which indicated the vibration modes of the O-H and –NH groups from enzymes that interact with nanoparticles, which has been suggested previously [19].

3.3 Operational stability of immobilised Phw and Psr

The operational stability in terms of temperature and pH is an important criterion in the application of immobilised enzymes [2,38]. To study this factor (Phw_im, Psr_im), various

pH values (5 – 11) and temperatures (~~30ºC 70ºC~~ 30 ºC – 70 ºC) were tested, and the results were compared with those of free enzymes (Phw_free, Psr_free). The results were analysed using analysis of variance (ANOVA) to indicate the significant factor influencing the stability of both enzymes. The ANOVA results in Table 1 show that the regression coefficients had a high statistical significance ($p<0.05$) and show the values obtained for the coefficient of determination for both Phw_im and Psr_im (R^2 0.9730 and R^2 0.9733) and Phw_free and Psr_free (R^2 0.9723 and R^2 0.9712, respectively). The values indicated that the model of the immobilised enzymes could not explain only 2.7% of the variables behaviour, while with the free enzymes the value was 2.8-2.9%. For immobilised enzymes, the calculated F-value (α=0.05, DOF=4,3) was 9.12 for the regression. This value was higher than the tabulated F-values (1.65, 1.85), indicating that the treatment differences were highly significant. Similarly, in free enzymes, the obtained F-values (2.90, 3.94) were less than the critical F-value ($F_{0.05(4,5)}$ = 5.19), reflecting the significance of the model. The following Equations (6 – 9) represent the second order polynomial model of the residual activity for the experimental data:

$$\text{Residual Phw\_im}(\%) = -407.2 + 56.5\text{pH} + 10.1\text{T} - 2.6\text{pH}^2 - 0.1\text{T}^2 - 0.16\text{pHT} \quad (6)$$

$$\text{Residual Psr\_im}(\%) = -275.9 + 41.8\text{pH} + 6.3\text{T} - 1.8\text{pH}^2 - 0.05\text{T}^2 - 0.17\text{pHT} \quad (7)$$

$$\text{Residual Phw\_free}(\%) = 22.2 + 2.5\text{pH} + 1.5\text{T} - 0.026\text{T}^2 \quad (8)$$

$$\text{Residual Psr\_free}(\%) = 66.4 + 1.04\text{pH} + 0.54\text{T} - 0.021\text{T}^2 \quad (9)$$

For free enzymes, the models were reduced by removing the interaction between pH and temperature, as it was not significant to the stability of the free enzymes.

Contour plots of the second order polynomial model were generated as a function of the independent variables of pH and temperature for immobilised and free enzymes. The contour plots of free Phw and Psr exhibited their stability under mesophilic conditions (~~30ºC~~ 30 ºC to ~~40ºC~~ 40 ºC). Free enzymes were stable over a broad range of pH values (Fig. 6b, 6d), with no

optimum condition obtained in the range tested (pH 5-11). However, both of the immobilised enzymes had improved the stability by achieving their optimum condition in the alkaline region (pH 8 to 11) with thermophilic temperature stability ranging from ~~40ºC~~ 40 ºC to ~~60ºC~~ 60 ºC for immobilised Phw (Fig. 6a) and ~~40ºC~~ 40 ºC to ~~55ºC~~ 55 ºC for immobilised Psr (Fig. 6c).

3.4 Storage stability of immobilised Phw and Psr

Storage stability plays a crucial role in the use immobilised proteases, as the shelf life determines the viability of an immobilised enzyme over time [39]. The storage stabilities of enzymes immobilised via a crosslinker (Phw_GA and Psr_GA) and adsorption (Phw_adsorp and Psr_adsorp) were tested by dispersing the immobilised enzymes in Tris buffer and maintaining them at ~~4ºC~~ 4 ºC for 60 days. Free enzymes (Phw_free and Psr_free) were used as controls to monitor the durability of enzyme activity. Phw_free and Psr_free were not stable in solution, as their activity decreased over time. This fact could be related to the behaviour of the proteases, as they tend to autolyse themselves by nucleophilic attack on the intermediate in a presence of water [1,40]. After 7 days of storage at ~~4ºC~~ 4 ºC, the residual activity of Phw_free and Psr_free was less than 17% (Table 2). There was a significant decrease in the activity of the immobilised enzyme via adsorption over 60 days of storage, with a residual activity of less than 45%. The weak bonding between the enzyme and nanoparticles could induce partial desorption during the period of storage. Generally, immobilisation via adsorption involves relatively weak interactions, such as electrostatic interactions, hydrogen bonds, van der Waals forces and hydrophobic interactions, which tend to strip off enzymes from the carrier easily, thus leading to a loss of activity and contamination of the reaction media [9]. However, the enzymes immobilised via crosslinking (Phw_GA and Psr_GA) retained 91% and 86% of their residual activity, respectively, after

60 days of storage at 4ºC (Table 2). These results show that enzymes immobilised created by crosslinking provide a distinctive advantage in stability over immobilised enzymes created by adsorption at a longer duration of storage.

3.5 Reusability of immobilised Phw and Psr

For the sake of the cost-effective use of enzymes, reusability is a critical factor to consider [41]. The reusability of immobilised Phw and Psr created using crosslinking was evaluated in a repeated batch process using fresh casein as a model protein in each batch cycle (Fig. 7). Both immobilised Phw and Psr retained 66% and 64% of their activity, respectively, after 7 cycles, indicating a significant enhancement of the stability of the crosslinking interaction between the proteases and nanoparticles. In this work, testing the reusability was feasible, as the immobilised enzymes were easily separated by a magnetic force.

3.6 Application of immobilised Phw and Psr in the hydrolysis of proteins

Casein has been used as a model protein to evaluate the degree of hydrolysis (DH) of immobilised enzymes created via crosslinking and free Phw or Psr. The results of the hydrolysis are shown in Fig. 8a. The DH of immobilised Phw (24%) was higher than that of free Phw (15%) during the first 30 min of reaction time (Fig. 8a). The maximum DH was achieved after 24 h and was 80% for immobilised Phw and 40% for free Phw. Besides, the residual activity of both immobilised Phw and Psr were stable for 24 h whereas the residual activity of free Phw and Psr had decreased pronouncedly after 24 h at 50 °C indicating an improvement of process efficiency and thermal stability of the immobilised enzymes [19]. The higher stability may be possibly due to the multipoint covalent binding of protease to the solid support that limit the flexibility and conformational mobility of the enzyme, hence inhibits unfolding or denaturation of the enzyme [42]. Likewise, the DH of immobilised Psr

(12%) showed the same rate as that of free Psr (13%) and continued to increase over time with a similar profile, reaching the maximum DH 30% in free Psr and 50% in immobilised Psr after 24 h of reaction time. Thus, the immobilised enzymes in the present study could enhance the ability of free enzymes to hydrolyse protein, as shown by the model protein, reflecting that the active enzymes were successfully immobilised.

The effect of both proteases (Phw and Psr) was also evaluated in hydrolysis of the protein source from animals (egg white albumin) and vegetables (oat bran protein isolate). The hydrolysis of oat bran protein isolate (OBPI) corroborated the efficiency of immobilised Phw and Psr, as they had a higher DH compared to free Phw and Psr over a longer duration (Fig. 8b). These results agree with those obtained using functionalized magnetite nanoparticles to hydrolyse soya protein isolates and whey protein isolates [29,43]. It seems that Psr exhibited a higher DH than (free and immobilised) Phw when using a vegetable protein source. In the hydrolysis of egg white albumin, immobilised Psr reached a maximum DH 60% after 24 h and free Psr achieved maximum DH 45% after 6 h, while Phw reached a maximum DH of 70% and 51% for immobilised and free Phw, respectively (Fig. 8c). Hence, the different source of the proteases seems to be a distinct behaviour that depends on the substrate source; in fact, it could determine the choice of enzymes according to the application, as suggested by others [2].

SDS-PAGE of the hydrolysates from selected proteins (casein, OBPI, egg white albumin) is shown in Fig. 9. The presence of several smaller peptides with low molecular weights support the idea that proteins were hydrolysed by immobilised protease derived from an animal source (Phw) and vegetable source (Psr). Similar profiles were obtained for both immobilised enzymes (Phw and Psr), showing their ability to perform the reaction after being grafted on nanoparticle surfaces created by crosslinking with glutaraldehyde.

4. Conclusion

Low-cost proteases obtained through the SSF of protein-rich wastes (hair waste and soya fibre residues) were successfully immobilised onto functionalized MNPs over a relatively short time. The ease of the separation and reusability of these enzymes in comparison with free enzymes could be considered an advantage of their use in industrial processes. Additionally, stability was enhanced from mesophilic to thermophilic conditions under alkaline conditions, preventing autolysis of the enzymes and maintaining their initial activities for 2 months with only 9%-14% activity loss. Immobilised Phw and Psr were able to hydrolyse some proteins derived from plant and animal sources with a high degree of hydrolysis, indicating that they are promising for immobilised enzyme applications in a wide range of industrial processes.

Acknowledgements

The authors thank the Spanish Ministerio de Economia y Competitividad (Project CTM2015-69513-R) for their financial support. N.A. Yazid thanks the Government of Malaysia and University Malaysia Pahang for their financial support. Raquel Barrena is grateful to TECNIOspring fellowship programme (no. TECSPR15-1-0051) co-financed by the European Union through the Marie Curie Actions and ACCIÓ (Generalitat de Catalunya).

References

[1] M.B. Rao, A.M. Tanksale, M.S. Ghatge, V. V Deshpande, Molecular and biotechnological aspects of microbial proteases., Microbiol. Mol. Biol. Rev. 62 (1998) 597–635.

[2] O.L. Tavano, Protein hydrolysis using proteases: An important tool for food biotechnology, J. Mol. Catal. B Enzym. 90 (2013) 1–11.

[3] A.K. Mukherjee, H. Adhikari, S.K. Rai, Production of alkaline protease by a thermophilic *Bacillus subtilis* under solid-state fermentation (SSF) condition using Imperata cylindrica grass and potato peel as low-cost medium: Characterization and application of enzyme in detergent formulation, Biochem. Eng. J. 39 (2008) 353–361.

[4] J. Abraham, T. Gea, A. Sánchez, Potential of the solid-state fermentation of soy fibre residues by native microbial populations for bench-scale alkaline protease production, Biochem. Eng. J. 74 (2013) 15–19.

[5] N.A. Yazid, R. Barrena, A. Sánchez, Assessment of protease activity in hydrolysed extracts from SSF of hair waste by and indigenous consortium of microorganisms, Waste Manag. 49 (2016) 420–426.

[6] S.S. Kim, H.S. Lee, Y.S. Cho, Y.S. Lee, C.S. Bhang, H.S. Chae, S.W. Han, I.S. Chung, D.H. Park, The effect of the repeated subcultures of Helicobacter pylori on adhesion, motility, cytotoxicity, and gastric inflammation., J. Korean Med. Sci. 17 (2002) 302–306.

[7] C. Mateo, J.M. Palomo, G. Fernandez-Lorente, J.M. Guisan, R. Fernandez-Lafuente, Improvement of enzyme activity, stability and selectivity via immobilization techniques, Enzyme Microb. Technol. 40 (2007) 1451–1463.

[8] M. Asgher, M. Shahid, S. Kamal, H.M.N. Iqbal, Recent trends and valorization of immobilization strategies and ligninolytic enzymes by industrial biotechnology, J. Mol. Catal. B Enzym. 101 (2014) 56–66.

[9] J. Xu, J. Sun, Y. Wang, J. Sheng, F. Wang, M. Sun, Application of iron magnetic nanoparticles in protein immobilization, Molecules. 19 (2014) 11465–11486.

[10] X. Jin, J.F. Li, P.Y. Huang, X.Y. Dong, L.L. Guo, L. Yang, Y.C. Cao, F. Wei, Y. Di Zhao, H. Chen, Immobilized protease on the magnetic nanoparticles used for the hydrolysis of rapeseed meals, J. Magn. Magn. Mater. 322 (2010) 2031–2037.

[11] I.A. Cavello, J.C. Contreras-Esquivel, S.F. Cavalitto, Immobilization of a keratinolytic protease from *Purpureocillium lilacinum* on genipin activated-chitosan beads, Process Biochem. 49 (2014) 1332–1336.

[12] H.J. Chae, M.J. In, E.Y. Kim, Optimization of protease immobilization by covalent binding using glutaraldehyde., Appl. Biochem. Biotechnol. 73 (1998) 195–204.

[13] S.A. Ansari, Q. Husain, Potential applications of enzymes immobilized on/in nano materials: A review, Biotechnol. Adv. 30 (2012) 512–523.

[14] P. Xu, G.M. Zeng, D.L. Huang, C.L. Feng, S. Hu, M.H. Zhao, C. Lai, Z. Wei, C. Huang, G.X. Xie, Z.F. Liu, Use of iron oxide nanomaterials in wastewater treatment: A review, Sci. Total Environ. 424 (2012) 1–10.

[15] A. Sahu, P.S. Badhe, R. Adivarekar, M.R. Ladole, A.B. Pandit, Synthesis of glycinamides using protease immobilized magnetic nanoparticles, Biotechnol. Reports. 12 (2016) 13–25.

[16] S.-L. Cao, X.-H. Li, W.-Y. Lou, M.-H. Zong, Preparation of a novel magnetic cellulose nanocrystal and its efficient use for enzyme immobilization, J. Mater. Chem. B. 2 (2014) 5522–5530.

[17] S. Cao, H. Xu, X. Li, W. Lou, M. Zong, Papain@magnetic nanocrystalline cellulose nanobiocatalyst: a highly efficient biocatalyst for dipeptide biosynthesis in deep eutectic solvents, ACS Sustain. Chem. Eng. 3 (2015) 1589–1599.

[18] S. Cao, Y. Huang, X. Li, P. Xu, H. Wu, N. Li, W. Lou, Preparation and Characterization of Immobilized Lipase from *Pseudomonas Cepacia* onto Magnetic Cellulose Nanocrystals, Sci. Rep. 6 (2016) 1–12.

[19] R. Sinha, S.K. Khare, Immobilization of halophilic *Bacillus* sp. EMB9 protease on functionalized silica nanoparticles and application in whey protein hydrolysis, Bioprocess Biosyst. Eng. 38 (2015) 739–748.

[20] S. Jodayree, Antioxidant activity of oat bran hydrolyzed proteins in vitro and in vivo, Doctoral Thesis, Ottawa, Ontario, 2014.

[21] T.G. Hu, J.H. Cheng, B.B. Zhang, W.Y. Lou, M.H. Zong, Immobilization of alkaline protease on amino-functionalized magnetic nanoparticles and its efficient use for preparation of oat polypeptides, Ind. Eng. Chem. Res. 54 (2015) 4689–4698.

[22] A. Abo Markeb, A. Alonso, A.D.A.D. Dorado, A. Sánchez, X. Font, Phosphate removal and recovery from water using nanocomposite of immobilized magnetite nanoparticles on cationic polymer, Environ. Technol. 3330 (2016) 1–14.

[23] R.A. Sheldon, S. Van Pelt, Enzyme immobilisation in biocatalysis: why, what and how, Chem. Soc. Rev. 42 (2013) 6223–6235.

[24] K. Alef, P. Nannipieri, Methods in applied soil microbiology and biochemistry - Enzyme activities, Academic Press, San Diego, 1995.

[25] O.H. Lowry, N.J. Rosebrough, A.L. Farr, R.J. Randall, Protein measurement with the Folin phenol reagent., J. Biol. Chem. 193 (1951) 265–275.

[26] M.P.C. Silvestre, H.A. Morais, V.D.M. Silva, M.R. Silva, Degree of hydrolysis and peptide profile of whey proteins using pancreatin, Brazilian Soc. Food Nutr. 38 (2013) 278–290.

[27] D.A. Cowan, R. Fernandez-Lafuente, Enhancing the functional properties of thermophilic enzymes by chemical modification and immobilization, Enzyme Microb. Technol. 49 (2011) 326–346.

[28] S. Prasertkittikul, Y. Chisti, N. Hansupalak, Deproteinization of natural rubber using protease immobilized on epichlorohydrin cross-linked chitosan beads, Ind. Eng. Chem. Res. 52 (2013) 11723–11731.

[29] S.N. Wang, C.R. Zhang, B.K. Qi, X.N. Sui, L.Z. Jiang, Y. Li, Z.J. Wang, H.X. Feng, R. Wang, Q.Z. Zhang, Immobilized alcalase alkaline protease on the magnetic chitosan

564 nanoparticles used for soy protein isolate hydrolysis, Eur. Food Res. Technol. 239
565 (2014) 1051–1059.

566 [30] H. Quanguo, Z. Lei, W. Wei, H. Rong, H. Jingke, Preparation and Magnetic
567 Comparison of Silane-Functionalized Magnetite Nanoparticles, 22 (2010) 285–295.

568 [31] J.A. Lopez, F. González, F.A. Bonilla, G. Zambrano, M.E. Gómez, Synthesis and
569 characterization of Fe3O4 magnetic nanofluid, Rev. Latinoam. Metal. Y Mater. 30
570 (2010) 60–66.

571 [32] M.R. Ladole, A.B. Muley, I.D. Patil, M.I. Talib, R. Parate, Immobilization of
572 tropizyme-P on amino-functionalized magnetic nanoparticles for fruit juice
573 clarification, J. Biochem. Tech. 5 (2014) 838–845.

574 [33] I.J. Bruce, T. Sen, Surface modification of magnetic nanoparticles with alkoxysilanes
575 and their application in magnetic bioseparations, Langmuir. 21 (2005) 7029–7035.

576 [34] M. Yamaura, R.L. Camilo, L.C. Sampaio, M.A. Macedo, M. Nakamura, H.E. Toma,
577 Preparation and characterization of (3-aminopropyl)triethoxysilane-coated magnetite
578 nanoparticles, J. Magn. Magn. Mater. 279 (2004) 210–217.

579 [35] D.L. Pavia, G.M. Lampman, G.S. Kriz, J.A. Vyvyan, eds., Introduction to
580 spectroscopy, 5th ed., Cengage Learning, United State of America, 2015.

581 [36] R.A. Bini, R.F.C. Marques, F.J. Santos, J.A. Chaker, M. Jafelicci, Synthesis and
582 functionalization of magnetite nanoparticles with different amino-functional
583 alkoxysilanes, J. Magn. Magn. Mater. 324 (2012) 534–539.

584 [37] P.E.G. Casillas, C.A.R. Gonzalez, C.A.M. Pérez, Infrared Spectroscopy of
585 Functionalized Magnetic Nanoparticles, in: T. Theophile (Ed.), Infrared Spectrosc. -
586 Mater. Sci. Eng. Technol., InTech, 2012: pp. 405–420.

587 [38] R.J.S. De Castro, H.H. Sato, Production and biochemical characterization of protease
588 from *Aspergillus oryzae*: An evaluation of the physical-chemical parameters using
589 agroindustrial wastes as supports, Biocatal. Agric. Biotechnol. 3 (2014) 20–25.

590 [39] A.G. Kumar, S. Swarnalatha, P. Kamatchi, G. Sekaran, Immobilization of high
591 catalytic acid protease on functionalized mesoporous activated carbon particles,
592 Biochem. Eng. J. 43 (2009) 185–190.

593 [40] R. Beynon, J.S. Bond, eds., Proteolytic enzymes: a practical approach, 3rd ed., Oxford
594 University Press, 2001.

595 [41] T. Chen, W. Yang, Y. Guo, R. Yuan, L. Xu, Y. Yan, Enhancing catalytic performance
596 of β-glucosidase via immobilization on metal ions chelated magnetic nanoparticles,
597 Enzyme Microb. Technol. 63 (2014) 50–57.

598 [42] R.K. Singh, Y.W. Zhang, N.P.T. Nguyen, M. Jeya, J.K. Lee, Covalent immobilization
599 of beta-1,4-glucosidase from *Agaricus arvensis* onto functionalized silicon oxide
600 nanoparticles, Appl. Microbiol. Biotechnol. 89 (2011) 337–344.

[43] E.M. Lamas, R.M. Barros, V.M. Balcao, F.X. Malcata, Hydrolysis of whey proteins by proteases extracted from *Cynara cardunculus* and immobilized onto highly activated supports, Enzyme Microb. Technol. 28 (2001) 642–652.

Tables

Table 1 Analysis of variance (ANOVA) for the response surface quadratic model for immobilised (Phw_im and Psr_im) and free (Phw_free and Psr_free) enzymes.

Protease	Source of variation	Sums of square	Degree of freedom	Mean square	F-value	Prob>F
Phw_im	Regression	12107.4	5	2421.5	50.47	<0.0001
	Residual	335.9	7	47.98		
	Pure error	150	4	37.5		
	Lack of fit	185.9	3	61.95	1.65	
	Total	12443.2	12			
Psr_im	Regression	5108.7	5	1021.7	50.99	<0.0001
	Residual	140.3	7	20		
	Pure error	58.8	4	14.7		
	Lack of fit	81.5	3	27.2	1.85	
	Total	5248.9	12			
Phw_free	Regression	3382.4	3	1127.5	105.4	<0.0001
	Residual	96.3	9	10.7		
	Pure error	20.8	4	5.2		
	Lack of fit	75.5	5	15.1	2.9	
	Total	3478.7	12			
Psr_free	Regression	6452.3	3	2150.8	101.1	<0.0001
	Residual	191.5	9	21.3		
	Pure error	32.3	4	8.1		
	Lack of fit	159.2	5	31.8	3.94	
	Total	6643.8	12			

Phw_im: R^2 0.9730, adj R^2 0.9537, pred R^2 0.8519
Psr_im: R^2 0.9733, adj R^2 0.9542, pred R^2 0.8260
Phw_free: R^2 0.9723, adj R^2 0.9631, pred R^2 0.9315
Psr_free: R^2 0.9712, adj R^2 0.9616, pred R^2 0.9224

Table 2 The storage stability of free and immobilised enzymes created via crosslinking with glutaraldehyde (GA) and via adsorption (adsorp) during 60 days of storage.

Enzymes	Initial activity (U/ml)	Final activity (U/ml)	Residual activity (%)
Phw_GA	501±72	458±51	91
Psr_GA	346±69	297±84	86
Phw_adsorp	190±15	77±9	41
Psr _adsorp	152±9	46±5	30
Phw_free	537±26	91±21[a]	17
Psr_free	358±29	42±3[a]	12

[a] The final activity was determined after 7 days of storage.
The standard deviation was calculated from 3 replicates.

669 **Figure captions**

670 **Fig. 1** The effect of the glutaraldehyde (GA) concentration and crosslinking time on the
671 activity recovery of (a) Phw and (c) Psr with 0% GA (simple adsorption) (■), 1% GA (▨),
672 2.5% GA (▩), and 5% GA (▧); enzyme loading per carrier of (a) Phw and (c) Psr with 0%
673 GA (simple adsorption) (—●—), 1% GA (—○—), 2.5% GA (—▼—), and 5% GA (—△—);
674 immobilisation yield of (b) Phw and (d) Psr with 0% GA (simple adsorption) (■), 1% GA (
675 ▨), 2.5% GA (▩), and 5% GA (▧); immobilisation efficiency of (b) Phw and (d) Psr
676 with 0% GA (simple adsorption) (—●—), 1% GA (—○—), 2.5% GA (—▼—), and 5% GA (
677 —△—) onto amino-functionalized MNPs.

678 **Fig. 2** TEM images at a magnification of 30,000x of (a) naked MNPs, (b) amino-
679 functionalized MNPs, (c) amino-functionalized MNPs after being immobilised with Phw, and
680 (d) amino-functionalized MNPs after being immobilised with Psr.

681 **Fig. 3** The electron diffraction images of (a) naked MNPs, (b) MNPs after the addition of
682 CTAB, (c) MNPs after surface modification with APTES, and (d) MNPs after the
683 immobilisation of the enzymes Phw and Psr.

684 **Fig. 4** The SEM images at 50.00 KX magnification of (a) naked MNPs, (b) amino-
685 functionalized MNPs, (c) amino-functionalized MNPs after being immobilised with Phw, and
686 (d) amino-functionalized MNPs after being immobilised with Psr.

687 **Fig. 5** The FT-IR spectra of (A) naked MNPs, (B) amino-functionalized MNPs, (C) amino-
688 functionalized MNPs after immobilisation of Phw, and (D) amino-functionalized MNPs after
689 immobilisation of Psr.

690 **Fig. 6** Contour plots of the residual activity (%) of the enzymes in terms of their operation
691 stability as a function of pH and temperature of (a) immobilised Phw, (b) free Phw, (c)
692 immobilised Psr, and (d) free Psr

693 **Fig. 7** The reusability of immobilised Phw (■) and immobilised Psr (▭) onto amino-
694 functionalized MNPs using casein as a model substrate for the hydrolysis reaction

695 **Fig. 8** The degree of hydrolysis of the selected protein hydrolysates obtained from the
696 hydrolysis of immobilised Phw (—○—), free Phw (—●—), immobilised Psr (—△—), and free Psr
697 (—▼—) with (a) casein; (b) oat bran protein isolate (OBPI); and (c) egg white albumin. The
698 residual activity of immobilised Phw (—□—), free Phw (—■—), immobilised Psr (—◇—) and
699 free Psr (—◆—) in 50 °C during 24h.

700 **Fig. 9** SDS-PAGE of the hydrolysates after reduction using 2-mercaptoethanol for selected
701 proteins before and after treatment with the immobilised proteases; (1) Molecular mass
702 marker; (2) casein; (3) egg white albumin; (4) hydrolysate from casein after treated with
703 immobilised Phw; (5) hydrolysate from egg white albumin after treatment with immobilised
704 Phw; (6) hydrolysate from OBPI after treatment with immobilised Phw; (7) hydrolysate from
705 casein after treatment with immobilised Psr; (8) hydrolysate from egg white albumin after
706 treatment with immobilised Psr; (9) hydrolysate from OBPI after treatment with Psr.

707

708

709

710

711

712

713

714

715

716

717

718 **Fig. 1**

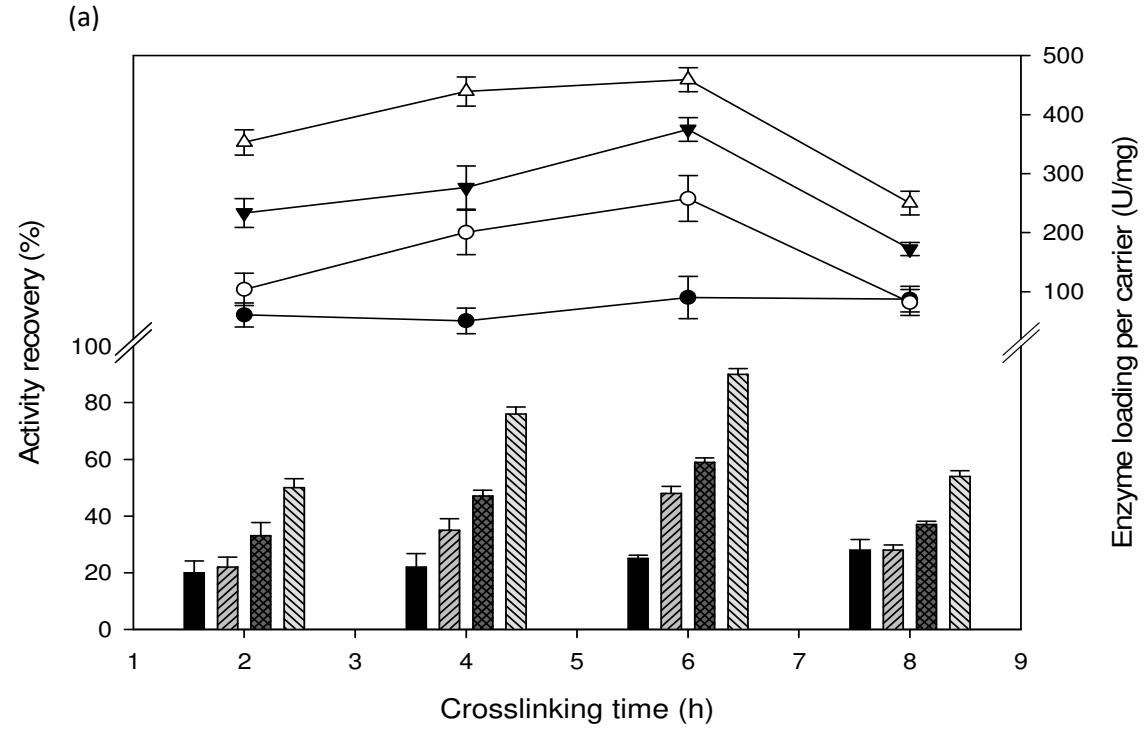

719

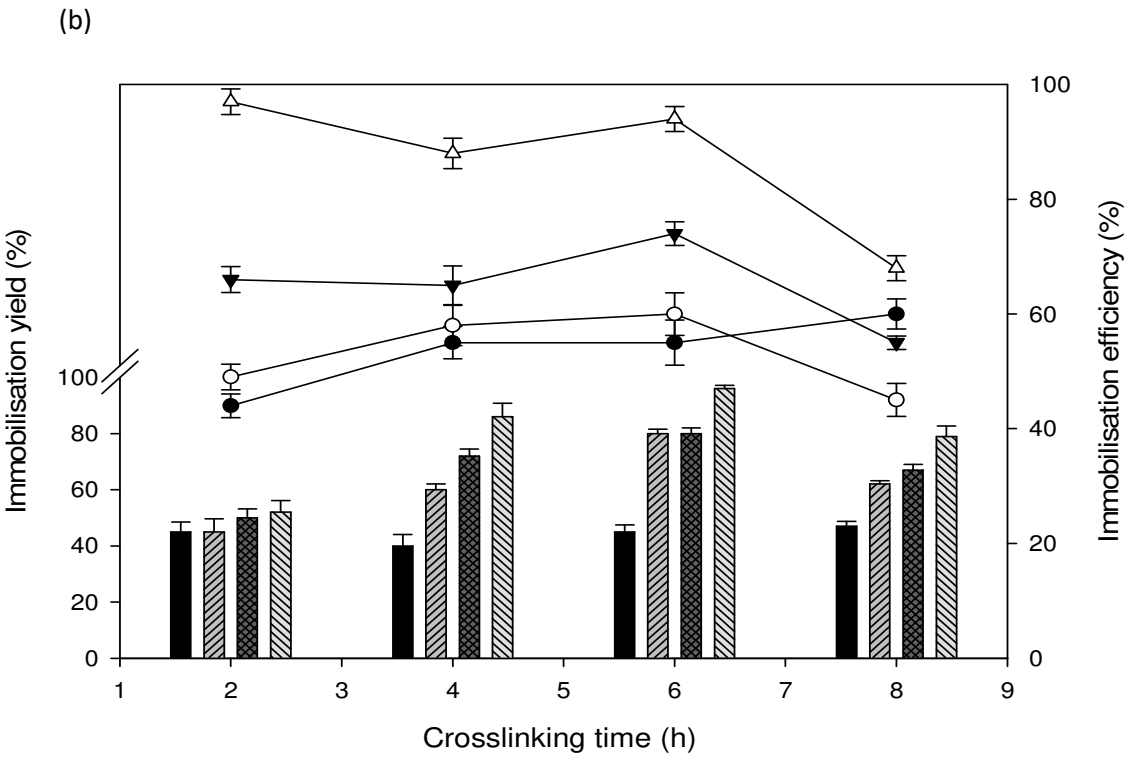

720

(c)

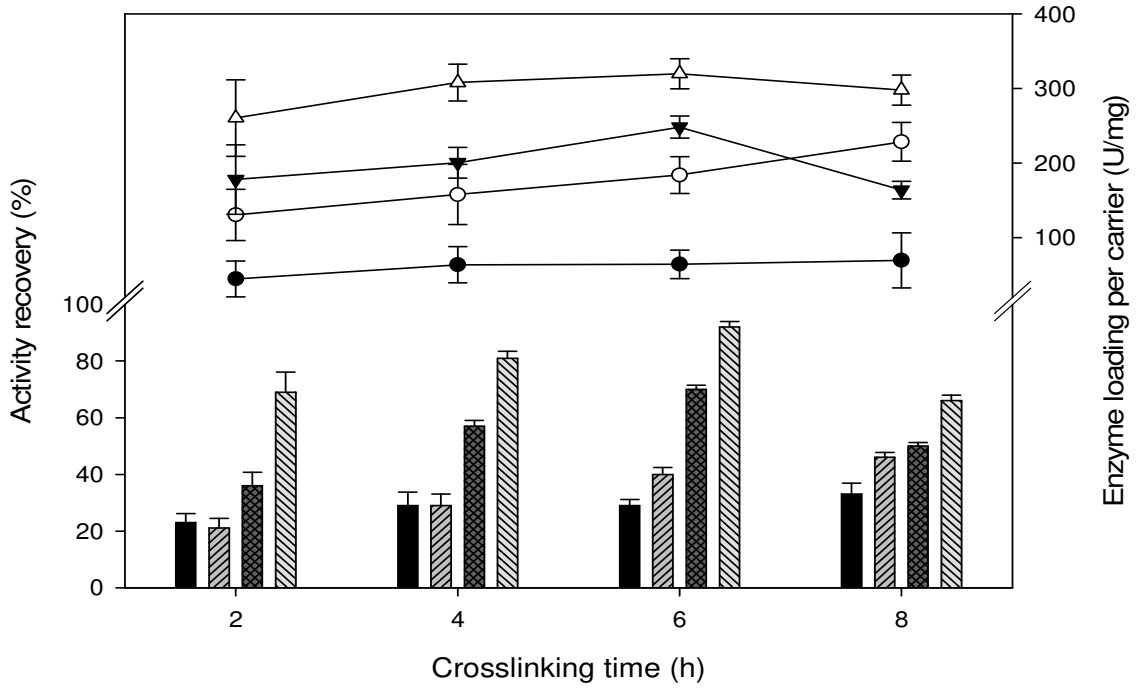

721

(d)

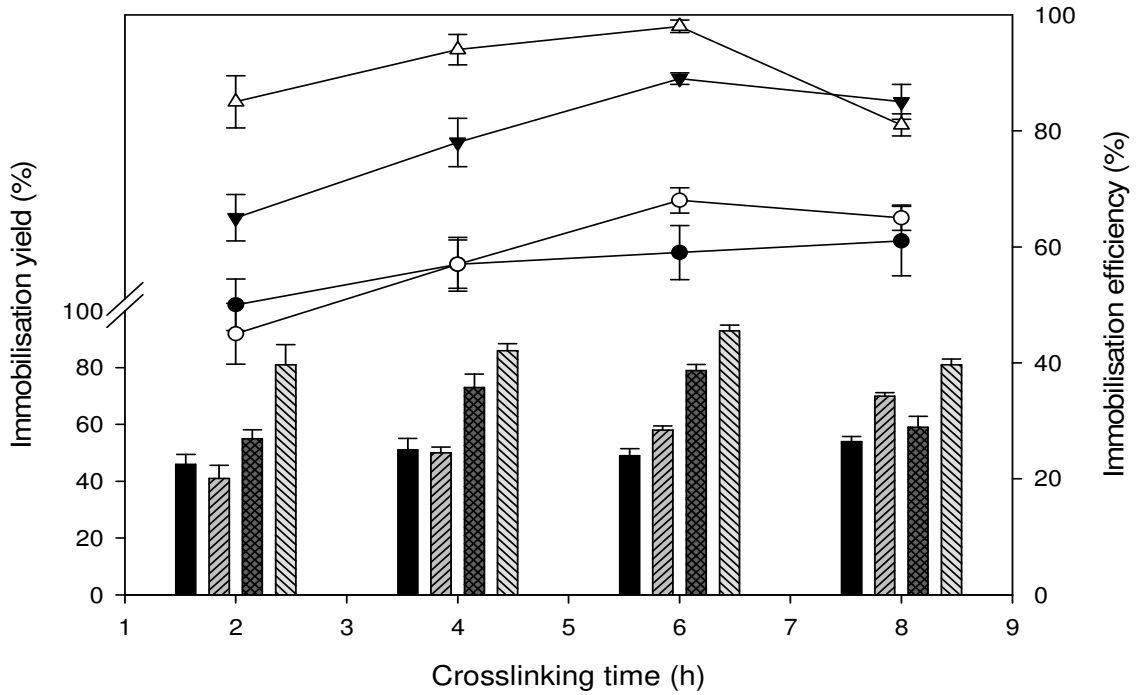

722

723

724

725

726

727 **Fig. 2**

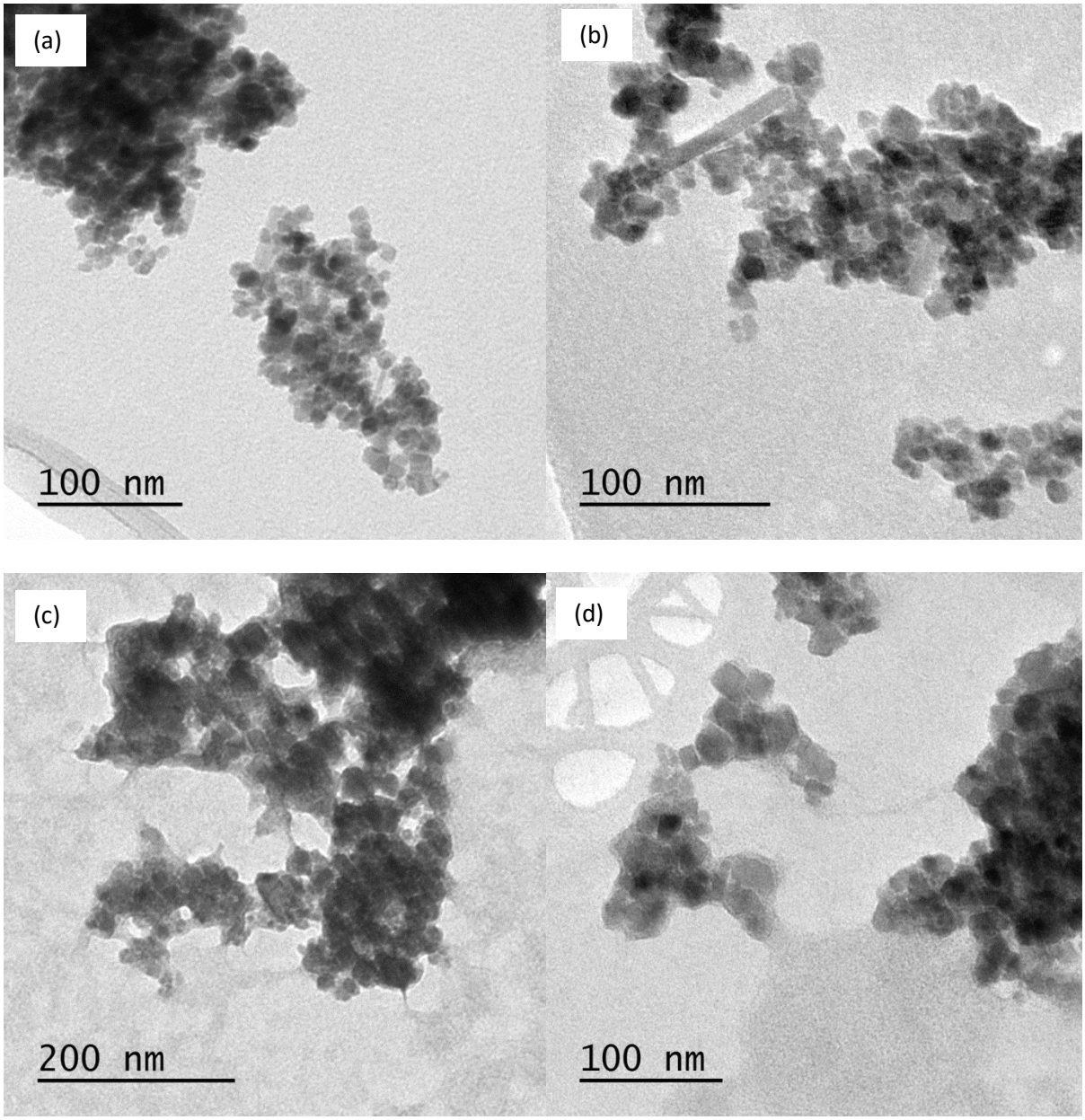

728

729

730

731

732

733

734

735

736

737 **Fig. 3**

738

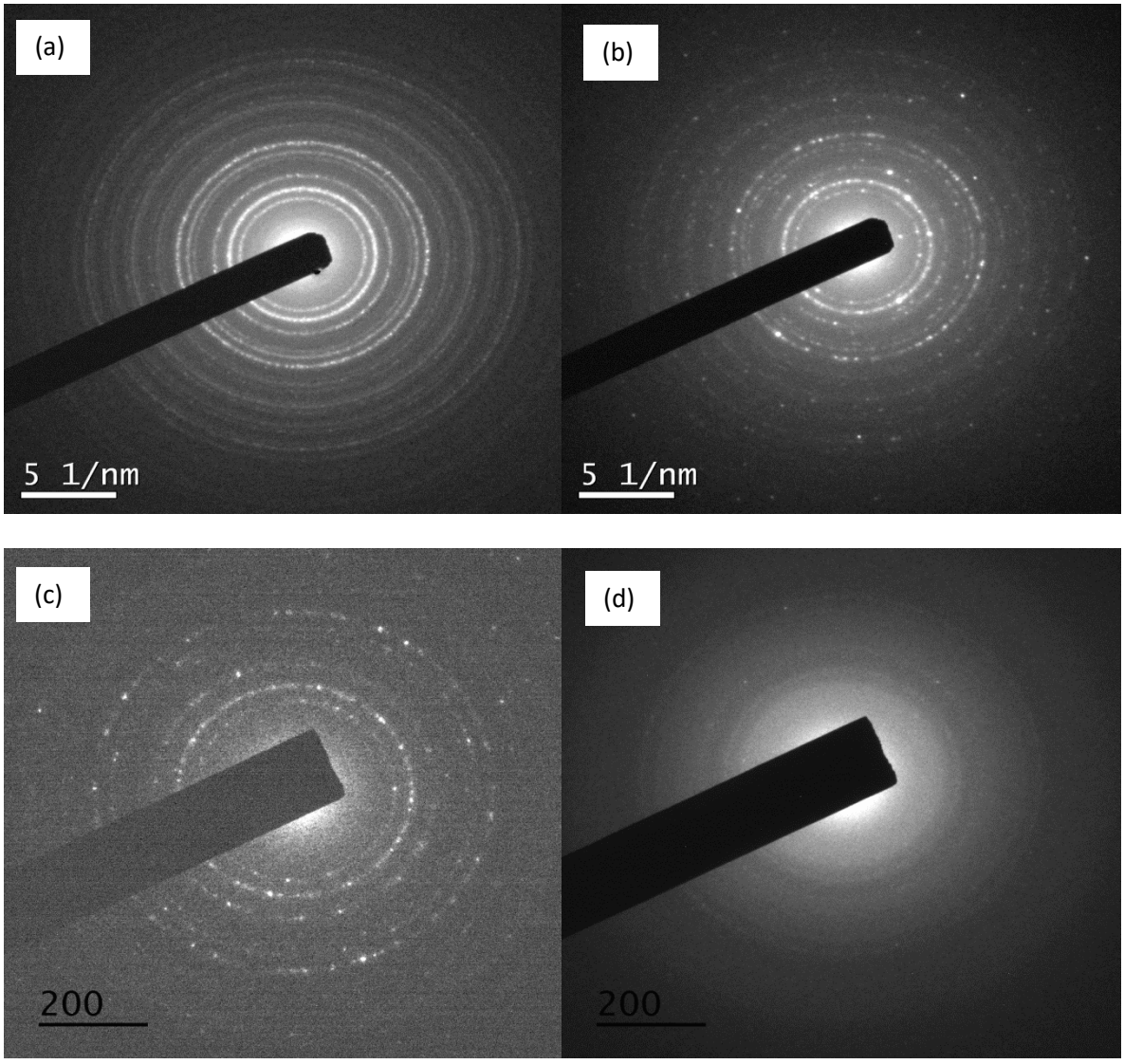

739

740

741

742

743

744

745

746

747

748

Fig. 4

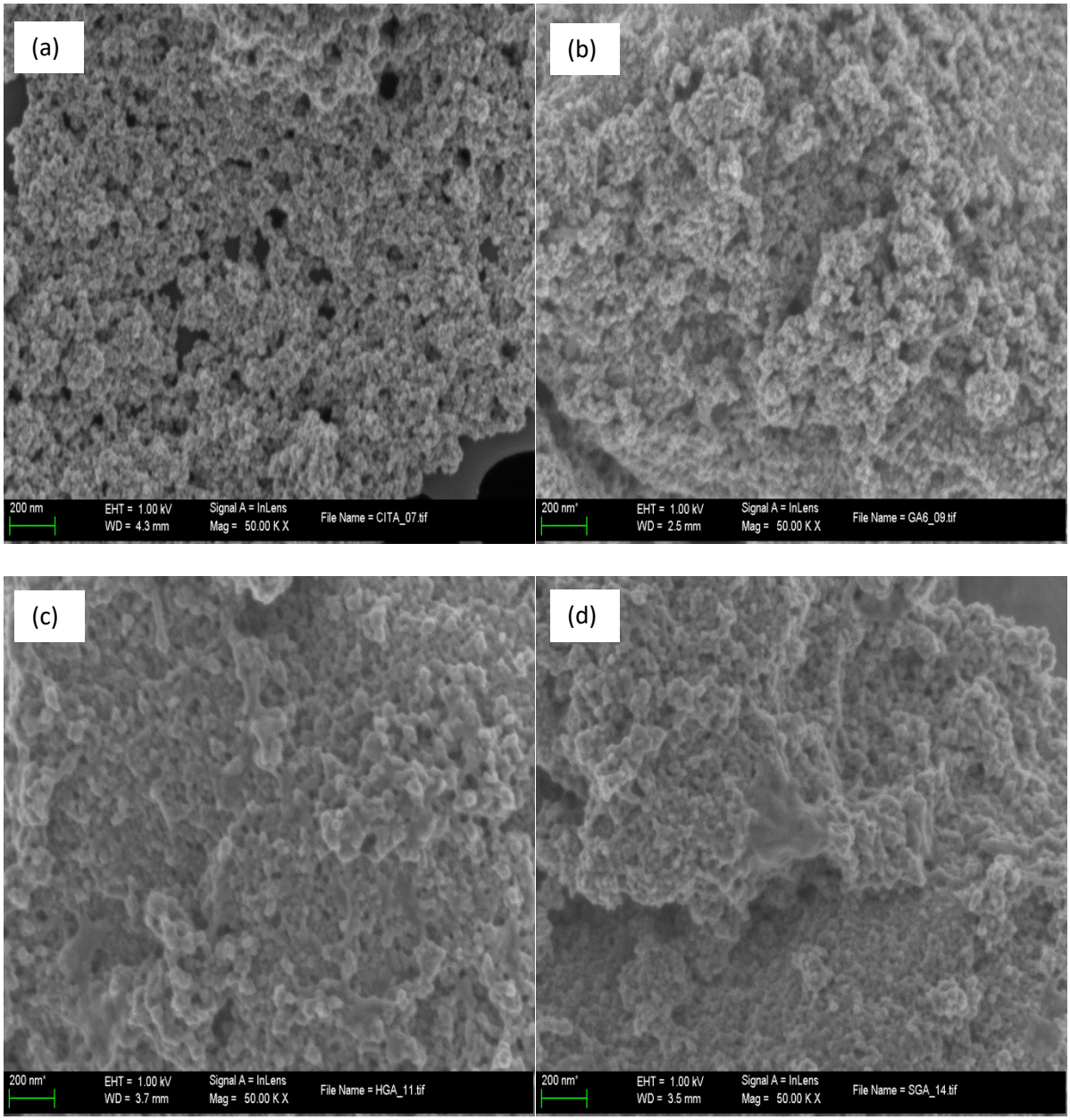
(a)
200 nm
EHT = 1.00 kV
WD = 4.3 mm
Signal A = InLens
Mag = 50.00 K X
File Name = CITA_07.tif
(b)
200 nm
EHT = 1.00 kV
WD = 2.5 mm
Signal A = InLens
Mag = 50.00 K X
File Name = GA6_09.tif
(c)
200 nm
EHT = 1.00 kV
WD = 3.7 mm
Signal A = InLens
Mag = 50.00 K X
File Name = HGA_11.tif
(d)
200 nm
EHT = 1.00 kV
WD = 3.5 mm
Signal A = InLens
Mag = 50.00 K X
File Name = SGA_14.tif

759 **Fig. 5**

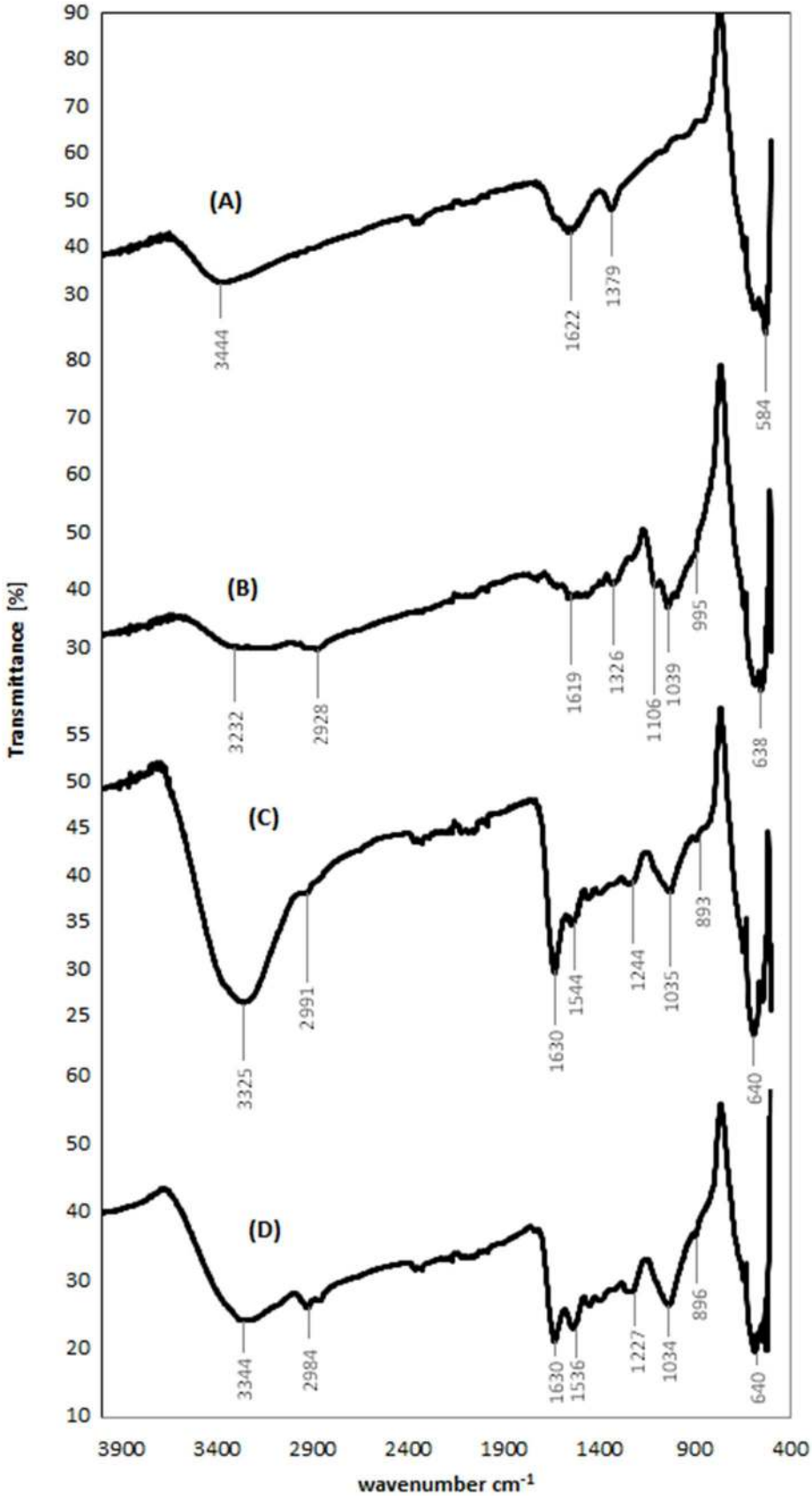

760

761

762 **Fig. 6**

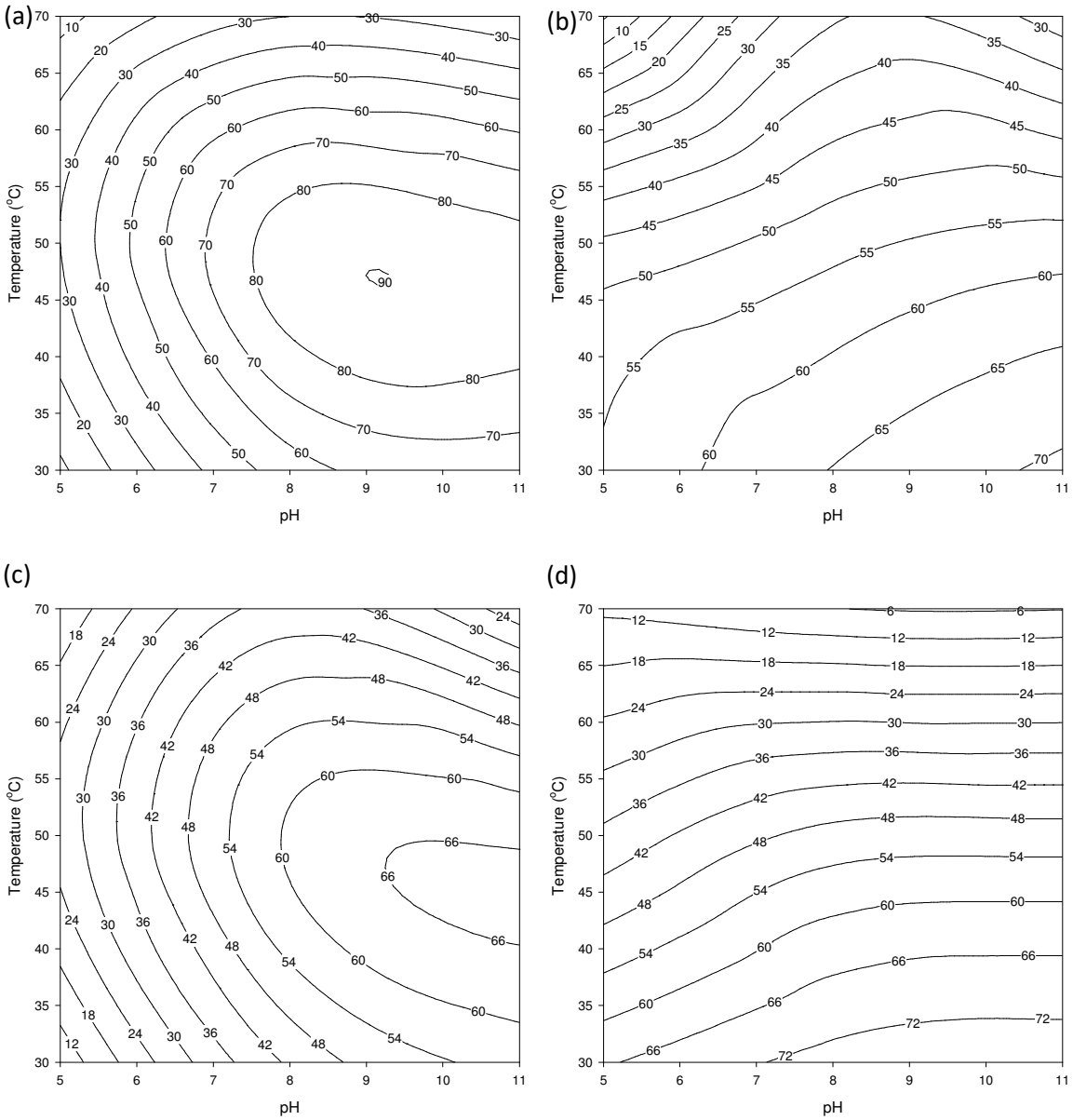

763

764

765

766

767

768

769

770

771

772 **Fig. 7**

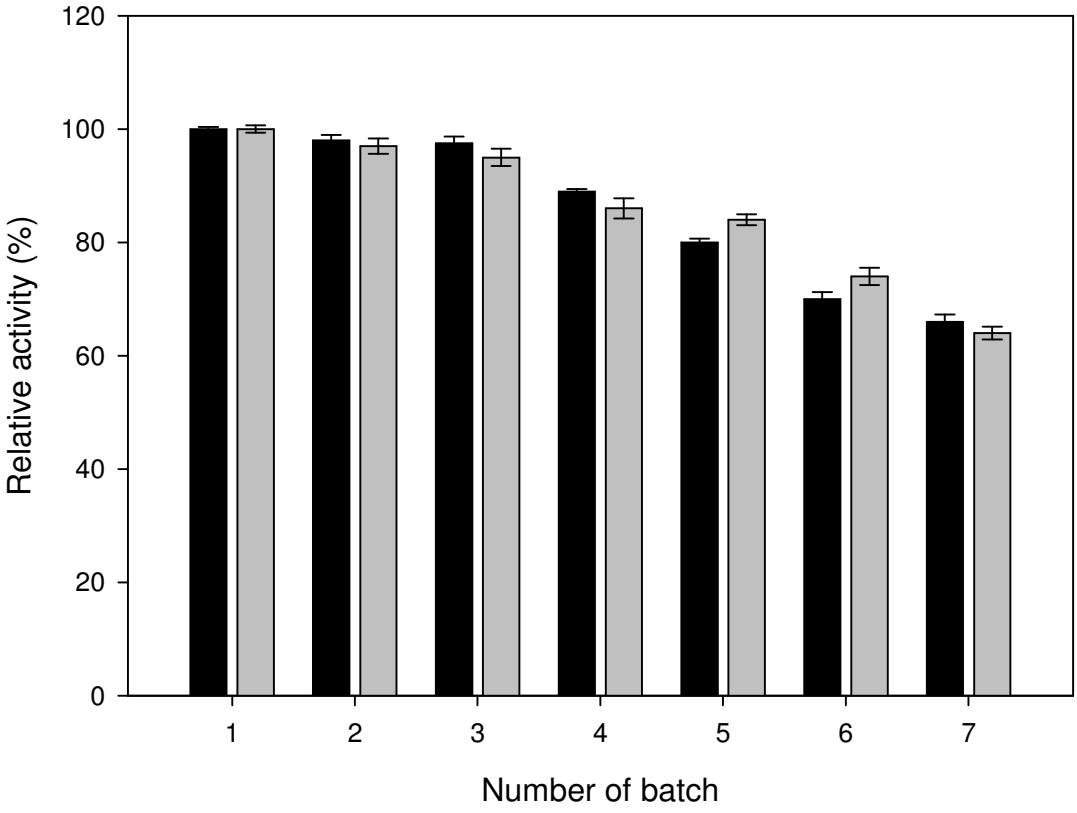

773

774

775

776

777

778

779

780

781

782

783

784 **Fig. 8**

(a)

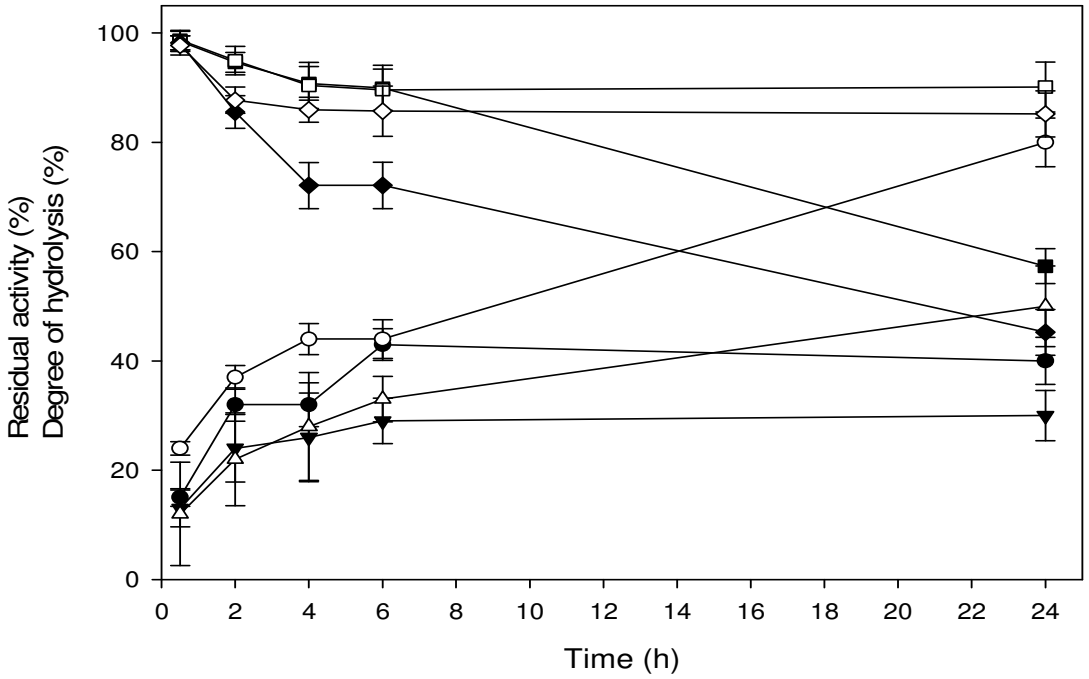

785

(b)

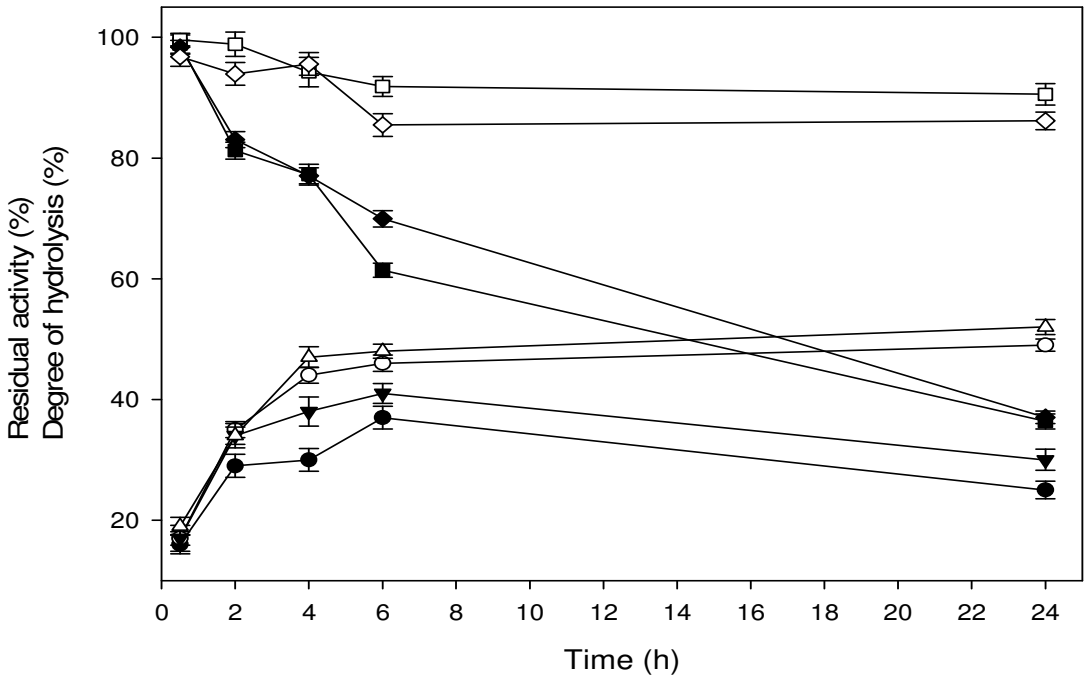

786

(c)

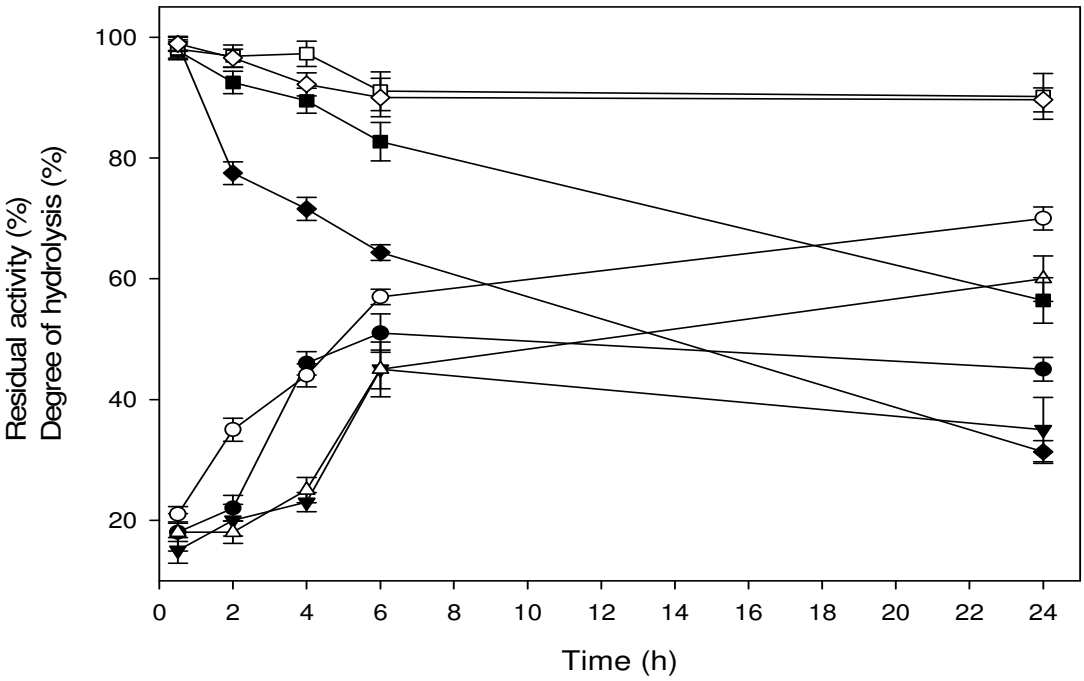

787

788

789

790

791

792

793

794

795

796

797

798

799

800

801

802 **Fig. 9**

803

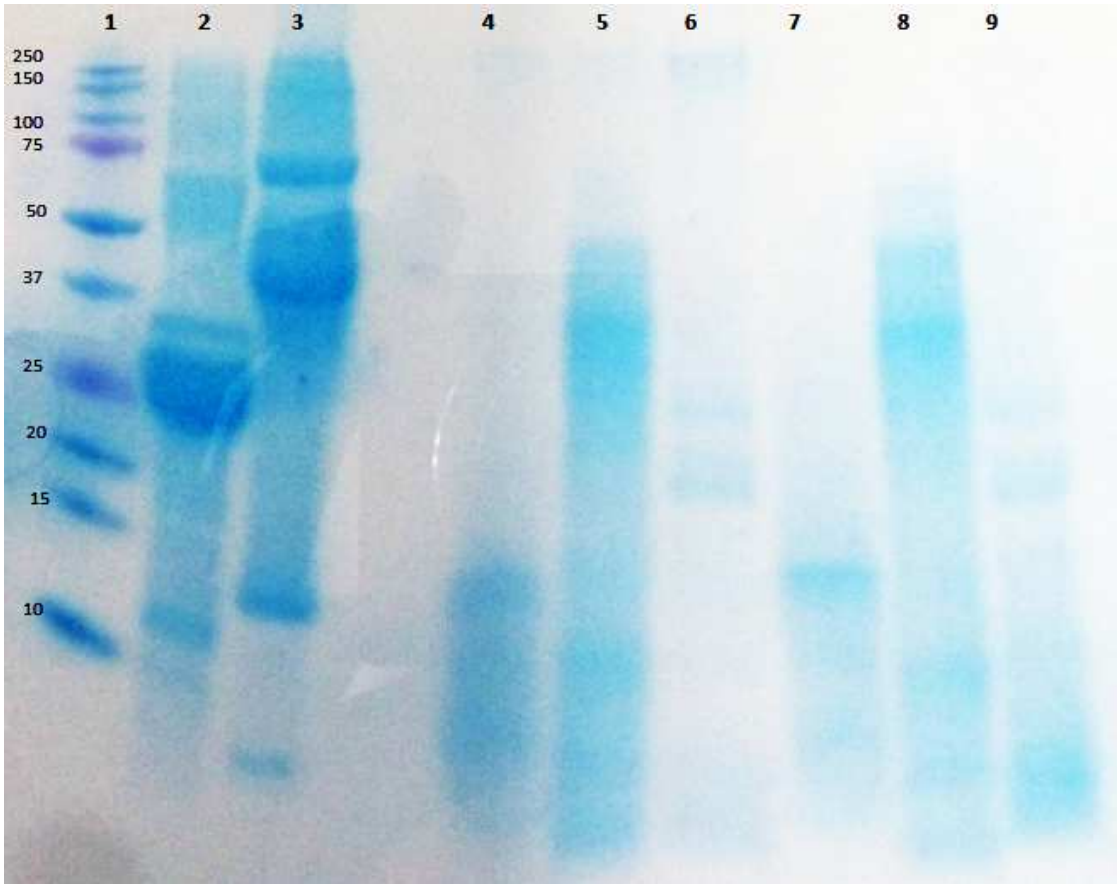

804